Published in final edited form as:
Biol Chem. 2014 September ; 395(9): 1003–1013. doi:10.1515/hsz-2014-0122.

Evolution of *Klk4* and enamel maturation in eutherians

Kazuhiko Kawasaki[a], **Jan C.-C Hu**, and **James P. Simmer**[*]
Department of Biologic and Materials Sciences, University of Michigan School of Dentistry, 1210 Eisenhower Place, Ann Arbor, MI 48108, USA

Abstract

Kallikrein-related peptidase 4 (*KLK4*) is a secreted serine protease that degrades residual enamel proteins to facilitate their removal by ameloblasts, which increases mineralization and hardens the enamel. Mutations in human *KLK4* cause hypomaturation amelogenesis imperfecta. Enamel formed by *Klk4* null mice is normal in thickness and prism structure, but the enamel layer retains proteins, is hypomineralized, and undergoes rapid attrition following tooth eruption. We searched multiple databases, retrieved *Klk4* and *Klk5* from various mammalian genomes, and identified *Klk4* in 47 boreoeutherian genomes. In non-Boreoeutheria, *Klk4* was detected in only one afrotherian genome (as a pseudogene), and not in the other six afrotherian, two xenarthran, or three marsupial genomes. In contrast, *Klk5* was detected in both marsupial and eutherian mammals. Our phylogenetic and mutation rate analyses support the hypothesis that *Klk4* arose from *Klk5* by gene duplication near the divergence of Afrotheria, Xenarthra and Boreoeutheria, and that functionally- differentiated *Klk4* survived only in Boreoeutheria. Afrotherian mammals share the feature of delayed dental eruption relative to boreoeutherian mammals. *KLK4* shortens the time required for enamel maturation and could have alleviated negative selection following mutations that resulted in thicker enamel or earlier tooth eruption, without reducing enamel hardness or causing dental attrition.

Keywords

Afrotheria; enamel; kallikrein-related peptidase 4; protease; tooth eruption

Introduction

Dental enamel is the hardest substance in the vertebrate skeleton, being 99% mineral by weight and 95% mineral by volume (Deakins and Volker, 1941). Its high degree of mineralization gives it the hardness of mild steel (Newbrun and Pigman, 1960). Enamel forms in stages (Lu et al., 2008). During the secretory stage, the enamel layer achieves its final dimensions, but the layer is soft and contains abundant protein in the spaces between the thin, ribbon-like crystals (Fukae and Shimizu, 1974). During the maturation stage

[*]**Corresponding author**: **James P. Simmer**, Department of Biologic and Materials Sciences, University of Michigan School of Dentistry, 1210 Eisenhower Place, Ann Arbor, MI 48108, USA, jsimmer@umich.edu.
[a]Present address: Department of Anthropology, Pennsylvania State University, University Park, PA 16802, USA

Supplemental Material: The online version of this article (DOI 10.1515/hsz-2014-0122) offers supplementary material, available to authorized users.

accumulated protein is removed and the crystals grow in width and thickness, eventually making contact and interlocking with adjacent crystals (Nanci, 2003). The thicker the enamel layer, the longer it takes to mature (harden) (Smith, 1998). For permanent human teeth (~ 2 mm), about 1000 days are devoted to enamel maturation. In contrast, mouse teeth have a thin enamel layer (~ 120 μm) that matures in about a week. The maturation of dental enamel is facilitated by kallikrein-related peptidase 4 (*KLK4*), which is secreted by transition and maturation stage ameloblasts (Hu et al., 2000, 2002; Simmer et al., 2011b) and cleaves enamel proteins into smaller peptides (Ryu et al., 2002; Nagano et al., 2009).

KLK4 is essential for the hardening of human and mouse enamel. Mutations in *KLK4* cause autosomal recessive hypomaturation amelogenesis imperfecta (Hart et al., 2004; Wang et al., 2013), a disorder having the principle phenotype of soft, stained enamel. *Klk4* null mouse teeth have soft enamel that is normal in thickness and enamel rod organization, but undergoes rapid attrition following tooth eruption (Simmer et al., 2009). Enamel proteins are retained in the *Klk4* null enamel layer even as the teeth erupt into function (Yamakoshi et al., 2011). *Klk4* null enamel is progressively less mineralized with depth (Hu et al., 2011; Smith et al., 2011) and tends to fracture near the dentino-enamel junction at the base of the enamel rods (Simmer et al., 2011a). The ability to remove protein from the matrix is not lost in *Klk4* null mice, just impaired. The sharp decline in matrix protein that normally occurs during early to mid maturation is reduced by half, with the superficial protein (that nearest to the ameloblast) being reabsorbed most efficiently. Despite the retention of proteins in the matrix, there is still a four-fold increase in mineralization (growth of enamel crystals in width and thickness) during early maturation; there is, however, only a 5% increase in mineralization thereafter, during mid to late maturation (Smith et al., 2011). Failure to fully remove protein from between the crystals prevents them from growing together and interlocking. This weakens the enamel rods, and the partially mature crystals can spill out of the rods in *Klk4* null mice (Simmer et al., 2009). These observations support the conclusion that *KLK4* cleaves enamel proteins to facilitate their reabsorption by ameloblasts, and that this activity is necessary to complete the maturation of dental enamel.

In humans there are 15 kallikrein genes, all clustered on the long arm of chromosome 19q13.33-q13.41 (Yousef et al., 2000). This *KLK* gene cluster is flanked by the *testicular acid phosphatase* (*ACPT*) and *SH3 and multiple ankyrin repeat domain 1* (*SHANK1*) genes on one end, and the *cytosolic thiouridylase subunit 1* (*CTU1;* also called cytoplasmic tRNA thiolation protein 1) and *sialic acid-binding immunoglobulin-type lectin type 9* (*SIGLEC9*) genes on the other. A similar cluster of continuous *KLK* genes is found in the genomes of most mammals. In our analysis, two discontinuous *KLK* gene clusters, split by a chromosomal rearrangement, were confirmed only in the opossum genome.

The *KLK* group is divided for historical reasons into the classical tissue kallikreins (*KLK1 – KLK3*) and the kallikrein-related peptidases (*KLK4 – KLK15*). With the exception of *KLK4*, orthologs of the 11 other human *kallikrein- related peptidase* genes were confirmed in marsupials in our study. The absence of *Klk4* in opossum may help explain an earlier observation that amelogenin in developing opossum enamel is largely intact (Ryu et al., 1998), and not in the state of partial degradation observed in mouse and porcine developing enamel. The unidentification of *Klk4* from marsupial genomes suggests that *Klk4* may be the

newest of the kallikrein-related peptidases, and raises the questions of when *Klk4* arose and how mammals lacking *Klk4* mature their enamel.

Class Mammalia comprises 5,419 or more extant species, which can be divided into three groups: Monotremata (egg-laying mammals; platypus and echidna), Marsupialia (marsupials), and Eutheria (placental mammals) (Wilson and Reeder, 2005; Madsen, 2009). Eutheria is further classified into three subgroups: Afrotheria, Xenarthra, and Boreoeutheria, see Table 1 (Murphy and Eizirik, 2009). Previous studies have suggested that Africa, South America, and Eurasia are the ancestral areas of Afrotheria, Xenarthra, and Boreoeutheria, respectively, and have correlated the separation of these three subgroups or the split of Afrotheria and Xenarthra with plate tectonic sundering (Wildman et al., 2007; Nishihara et al., 2009; Springer et al., 2011). Unfortunately, the phylogenetic relationship of these three groups has not been well resolved (Meredith et al., 2011; Song et al., 2012; O' Leary et al., 2013; Romiguier et al., 2013). This is mainly because these three lineages separated in a short period of time, which could result in disagreement of gene trees with species trees (Nei, 1987). In the present study, we investigated genome sequences in the databases, and identified *Klk4* in various boreoeutherian species. In non-Boreoeutheria, however, we detected only portions of a non-functional *Klk4* pseudogene in one of afrotherian species, *Chrysochloris asiatica* (Cape golden mole), and no *Klk4* in the other species of Afrotheria, Xenarthra, Marsupialia, Monotremata, or non-mammals. These results suggest that *Klk4* arose in Eutheria near the divergence of Afrotheria, Xenarthra and Boreoeutheria, and that *Klk4* remains functional only in extant Boreoeutheria.

Results

The *KLK* family

We identified *KLK* genes in the genome sequences of various mammals, birds, reptiles and the Western clawed frog. In Monotremata, the genome sequence was available for *Ornithorhynchus anatinus* (duckbilled platypus). This sequence was highly fragmented in the region around the *KLK* genes, however, and the entire active protease sequence was not detected in any of the platypus *KLK* genes. For this reason, platypus *KLK* genes were not included in our phylogenetic study, although various *KLK*-like sequences have been used in previous studies (Pavlopoulou et al., 2010; Koumandou and Scorilas, 2013).

In non-mammalian species, we identified six different apparently functional *KLK* genes in *Anolis carolinensis* (green anole lizard; *Klkac1 – Klkac6* in Figure 1), two in *Python bivittatus* (Burmese python), 11 in *Alligator sinensis* (Chinese alligator), 12 in *Pelodiscus sinensis* (Chinese softshell turtle), four in *Falco cherrug* (saker falcon; the largest number found in bird genomes), and six in *Xenopus tropicalis* (western clawed frog) genomes (*Klkxt1 – Klkxt6* in Figure 1; gene names used in different studies are summarized in Figures S1 and S2). Notably, most of these *KLK* genes are clustered in the genome, although some clusters are separated by sequence gaps (Figure S3). Furthermore, *Ctu1* is located adjacent to some *KLK* genes in the lizard, python and alligator genomes, similar to the arrangement of these genes in various mammalian genomes. This genomic arrangement corroborates our assignment of these genes as being members of the *KLK* gene family. Among the frog *KLK* genes, part of *Klkxt2* and *Klkxt3* localized in sequence gaps, so these genes were excluded

from our phylogenetic analysis. The discrepancy in the number of frog *KLK* genes in our study and a previous study (Koumandou and Scorilas, 2013) is mainly due to the difference in the genomic sequence used for the analysis and in the assignment of *KLK* and trypsin genes (see below). We also searched for *KLK* genes in teleost fish and the coelacanth using amino acid sequences coded by human *KLK* genes as queries, but only trypsin genes were detected (data not shown).

A phylogenetic tree was constructed showing the evolutionary relationships of the *KLK* genes (Figure 1). To clarify the early evolutionary history of human *KLK* genes, we paid special attention to *KLK* genes in Marsupialia, including *Monodelphis domestica* (gray shorttailed opossum), *Sarcophilus harrisii* (Tasmanian devil), and *Macropus eugenii* (tammar wallaby). *Klk6* and *Klk10* were detected in the opossum genome in a previous study (Elliott et al., 2006) but were not detected either in our study or in a study by others (Koumandou and Scorilas, 2013), although all or part of these two genes were identified in the wallaby (Koumandou and Scorilas, 2013). In this analysis, we chose *KLK* genes in the lizard as the reptile and bird representative. Our phylogenetic tree revealed that, among 15 human *KLK* genes, 11 (*Klk5 – Klk15*) have a marsupial ortholog, each connected by branches with high statistical support (99 –100% bootstrap value). The high bootstrap values obtained from phylogenetically distant mammalian species indicate distinct amino acid sequences encoded by the *Klk5 –Klk15* genes.

In non-mammalian *KLK* genes, two lizard genes, *Klkac3* and *Klkac4*, were placed within the large mammalian *KLK* gene clade (Figure 1). However, branches connecting these lizard genes or any other non-mammalian genes with mammalian *KLK* clades were not statistically supported (≤ 33 %). We were therefore unable to detect any lizard or frog *KLK* gene that is orthologous to a mammalian *KLK* gene or a common ancestor of two or more mammalian *KLK* genes. The same result was also obtained when we added alligator, turtle, python and bird *KLK* genes (Figure S4). The phylogenetic distribution of orthologous genes suggests that most of the 15 human *KLK* genes arose in Synapsida (including mammals) after the divergence from Sauropsida (including reptiles and birds) but before the divergence of Eutheria and Marsupialia. In our study, however, none of *Klk1*, *Klk2*, *Klk3* and *Klk4* were identified in Marsupialia, consistent with the findings of a previous study (Lundwall, 2013). One or more of these four genes likely arose more recently in Eutheria, as previously suggested for *Klk2*, *Klk3* and *Klk4* (Pavlopoulou et al., 2010).

Klk4 onset in mammals

Our phylogenetic tree reveals reliable clustering of *KLK4* and *KLK5* (97 %), supporting their close evolutionary relationship. In addition, *KLK4* is located immediately downstream of *KLK5* in the genome of humans and various other mammals (data not shown). Given the high sequence similarity between *KLK4* and *KLK5* and their close proximity within the *KLK* gene cluster, we made a comprehensive search for these genes throughout the databases. As a result, apparently functional *Klk4* was identified in 47 species, and was exclusively found in Laurasiatheria and Euarchontoglires, both consisting of Boreoeutheria (Table 1).

Among these boreoeutherian species, 24 different *Klk4* genes (including eight pseudogenes) were identified in the *Chinchilla lanigera* (long tailed chinchilla) genome and 14 *Klk4* genes (including four pseudogenes) in the *Octodon degus* (common degu; Table S1) genome. These genes are clustered in two different contigs in both species. However, one end of these two contigs ends up with a sequence gap, while the other end is flanked by *Klk5* in one contig and *Klk15* in the other (Table S1). These arrangements strongly suggest that all these *Klk4* genes in both species are clustered between *Klk5* and *Klk15*, similar to *Klk4* in other boreoeutherian species. Importantly, these genes can be phylogenetically classified into two different clades (Figure S5). A single gene immediately downstream of *Klk5* is more closely related to *Klk4* of the other species, and we refer to this gene as *bona fide Klk4* By contrast, all the other *Klk4* (*Klk4 - like*) genes in both species form a single clade, different from *bona fide Klk4* genes (98% bootstrap value). This result suggests that the initial *Klk4 - like* genes arose in the common ancestor of the chinchilla and degu, and rapidly differentiated from *bona fide Klk4*, the process probably being similar to *Klk4* and *Klk5*, as we will describe below. Subsequently, the *Klk4 - like* gene underwent reiterated gene duplication that resulted in many lineage-specific genes. As these *Klk4 - like* genes appear to have diverged asymmetrically from *bona fide Klk4*, we excluded *Klk4 - like* genes from the following analysis about early evolution of *Klk4* and *Klk5* .

In order to confirm the narrower phylogenetic distribution of *Klk4*, we intensively searched for evidence of *Klk4* in the genome of non-boreoeutherian species. As a result, exons 4 – 6 of *Klk4* were identified in the golden mole (Afrotheria) genome in a region immediately downstream of *Klk5*, similar to the boreoeutherian orthologs. However, all these exons were highly fragmented and had two termination codons (Figure S6). We thus concluded that this is a decaying pseudogene. No *Klk4* was detected in the genome of the six other afrotherian, two xenarthran or three marsupial species currently available in the database (Table 1). By contrast, *Klk5* is phylogenetically more widely distributed than *Klk4* and was discovered in 62 species, including Boreoeutheria, Xenarthra, Afrotheria and Marsupialia (exon 4 of a *Klk5 - like* gene was detected in the platypus genome sequence, but was not confirmed by our phylogenetic analysis, because of its small size; (Table 1). Based upon the phylogenetic distribution of *Klk4* and *Klk5* and upon the phylogenetic history of Mammalia, it is likely that *Klk4* arose from *Klk5* in Eutheria near the divergence of Afrotheria, Xenarthra and Boreoeutheria, although functional *Klk4* has been identified only in boreoeutherian species.

Functional divergence of *Klk4* and *Klk5*

Using these *Klk4* and *Klk5* sequences, we constructed a more inclusive phylogenetic tree for these two genes (closely related *Klk7* was used for the outgroup; Figure 2A). The result corroborates the tree shown in Figure 1, indicating that all *Klk4* and *Klk5* genes formed two different clades, each supported by a 99% or 100% bootstrap value. The complete separation of the *Klk4* clade from the *Klk5* clade that comprises genes in both Eutheria and Marsupialia appears to suggest that the origin of *Klk4* is older than the divergence of these two mammalian groups. However, this topology could be also explained if *Klk4* functionally differentiated from *Klk5*. While *Klk5* maintained its original functions after the duplication, *Klk4* may have obtained novel functions, hence a new sequence, as expected from the classical gene duplication model (Ohno, 1970). The new sequence would be subject to

different functional constraints (acceptable amino acid changes) from the original ones. As a result, *Klk4* and *Klk5* may have maintained distinct sequences, even though *Klk4* arose from *Klk5* relatively recently.

Based upon the multiple amino acid sequence alignment used to construct the phylogenetic tree (Figure 2A), we estimated the coefficient of type-I functional divergence (θ; see Materials and methods) between *Klk4* and *Klk5* as the probability that the evolutionary rate at each site is statistically independent between the two gene clades (that is, the two genes are subject to different functional constraints) (Gu, 1999). The estimated θ between *Klk4* and *Klk5* was 0.555 ±0.040 (Table 2), which rejects the null hypothesis ($\theta = 0$) that the evolutionary rate of these two genes is virtually the same at all amino acid positions. The coefficient of type-II functional divergence was also estimated, but was not significant (data not shown).

The significant pairwise θ value estimated between *Klk4* and *Klk5* does not reveal the extent of changed evolutionary rates in each gene. Based upon the θ values between the *Klk4*, *Klk5* and *Klk7* clusters (Table 2), however, it is possible to estimate the type-I functional branch length of each *KLK* gene cluster from their common ancestral gene (the branch length to the *Klk4*, *Klk5* and *Klk7* clusters is represented by b4, b5 and b7, respectively; Figure 2B) (Wang and Gu, 2001). The estimated branch length is extremely small for *Klk5* (b5 = 0.062) and large for both *Klk4* and *Klk7* (b4 = 0.641 and b7 = 0.546). This result indicates that the evolutionary rate of each site in *Klk5* is similar to the ancestral gene. By contrast, *Klk4* (and *Klk7*) appears to have an evolutionary rate that is greatly altered from the ancestral gene. Taken together, our results suggest that *Klk4* and *Klk5* have diverged functionally since their duplication, and that this functional divergence is mainly attributable to differentiation of *Klk4* from *Klk5*, which appear to have inherited the ancestral functions.

Given the result suggesting the possibility of asymmetrical type-I functional divergence of *Klk4* from *Klk5*, we assessed positions that potentially contributed to this divergence by calculating the posterior probability of the shift in the evolutionary rate at each position (Gu, 1999). Among the 217 positions tested, 98 positions showed $p > 0.5$, including 65 positions with $p > 0.67$ (Figure S7) with twice the probability of a shift (Wang and Gu, 2001). The high ratio of these positions observed in *Klk4* and *Klk5* ($p>0.5$ for 45.2% and $p > 0.67$ for 30.0% of the total positions) suggests altered functional constraints for these two genes, and provides further statistical evidence for a type I functional divergence.

The positions that potentially contributed to the functional divergence of *KLK4* and *KLK5* include four positions, 94, 188, 209 and 219, each supported by an extremely high probability ($p > 0.93$; Figure S7). At these positions, *KLK5* in all species studied has His, Gln, Asp and Gly residues, respectively, whereas these amino acids were not found (at positions 94, 188 and 209) or not predominant (at 219) in *KLK4*. Remarkably, all of these residues in *KLK5* were suggested to directly associate with or to regulate access to the cleavage site of substrates (Debela et al., 2007, 2008). *KLK5* is known to exhibit a strong P1-Arg preference (cleave sites C-terminal to an Arg residue) among various kallikrein-related peptidases (Debela et al., 2006). It is thus possible that relaxed constraints at these

four positions in *KLK4* led a functional divergence from *KLK5*, such as a broader substrate specificity to enamel matrix proteins.

Discussion

Early evolution of *KLK* genes before the origin of *Klk4*

The human *KLK* family is encoded by a contiguous cluster of *KLK* genes that is not interrupted by non- *KLK* genes, which enables evolutionary studies to learn about the timing of gene duplication events (Pavlopoulou et al., 2010; Koumandou and Scorilas, 2013; Lundwall, 2013). These evolutionary analyses depend, of course, on the quality of the genome sequences available from species that diverged shortly before and after the gene duplication of interest, as well as selection pressure to maintain the genes' integrity. No *KLK* genes have been identified in teleosts (Wong and Takei, 2013) or the coelacanth. The first *KLK* gene may have arisen in the tetrapod lineage. *Klk15* (NM_001011435.1) was reportedly found in the frog genome (Klein et al., 2002). Our phylogenetic analysis, however, showed that this gene and an adjacent gene (*cationic trypsin-3-like;* XM_004920289.1) in the frog genome formed a cluster with trypsin genes, with significant statistical support (97% boot strap value), but not with *KLK* genes (Figure S4). Although a previous study (Koumandou and Scorilas, 2013) also obtained a similar result, these authors regarded these and other *trypsin-like* genes as *KLK* genes. By contrast, we consider these genes to be trypsin genes based upon sequence similarities. Unlike the study by Koumandou and Scorilas (2013), in a genomic region upstream of these two trypsin genes, we identified three genes, *synaptotagmin 3* (*Syt3*), *Shank1*, and *ER membrane protein complex subunit 10* (*Emc10*; Figure S3). All of these genes are located near the *KLK* gene cluster in the human and various other mammalian genomes. The arrangement of these genes strongly suggests that *KLK* genes differentiated from a *trypsin* or *trypsin-like* gene. This proposition is supported by the fact that the amino acid sequences coded by *KLK* genes show the highest sequence similarities to trypsins among various serine proteases. Furthermore, the relative position of the four introns with respect to the encoded protein sequence and the phase of these introns (location of an intron within a triplet or between two adjacent triplets) are all identical in *KLK* genes and trypsin genes, but different in other serine protease genes. The close amino acid sequences encoded by *KLK* and *trypsin* genes validate the use of *trypsin* genes as the outgroup in our phylogenetic analysis (Figure 1). Within mammals, each of the 12 *kallikrein-related peptidase* genes separated in phylogenetic analyses into a distinct monophyletic group, suggesting that each has adopted a separate and necessary function (Koumandou and Scorilas, 2013).

Evolution of *Klk4* in mammals

Our phylogenetic analyses support the findings of others that *Klk4* was spawned by a duplication of *Klk5* (Elliott et al., 2006), which is adjacent to *Klk4* and in the same orientation on the *KLK* locus. Our analysis further suggested that *Klk4* and *Klk5* have functionally diverged since their duplication, and that *Klk4* is the gene that adopted a new function. We used the close connection between *Klk4* and *Klk5*, both physically on the *KLK* locus and evolutionarily, to search genome databases for the presence of these two genes. Although *Klk5* is found in Marsupialia, *Klk4* is not. We were able to identify *Klk5* in the

gray short-tailed opossum, tammar wallaby and the Tasmanian devil (and possibly in the platypus) genomes. Furthermore, we were able to detect only a highly fragmented pseudogene of *Klk4* in the golden mole genome but were not able to identify any evidence of *Klk4* in the genomes of six other afrotherian mammals in separate orders and two xenarthran mammals, including the lesser hedgehog tenrec (*Echinops telfairi*), elephant shrew (*Elephantulus edwardii*), aardvark (*Orycteropus afer*), African bush elephant (*Loxodonta africana*), rock hyrax (*Procavia capensis*), West Indian manatee (*Trichechus manatus latirostris*), Hoffmann' s two-toed sloth (*Choloepus hoffmanni*), and nine-banded armadillos (*Dasypus novemcinctus*). By contrast, *Klk5* was identified in all these afrotherian and xenarthran species. These findings support and expand upon similar findings by others (Pavlopoulou et al., 2010; Lundwall, 2013). In addition, we identified apparently functional *Klk4* in 47 out of 52 boreoeutherian genomes, including many representatives of both clades of Boreoeutheria: Euarchontoglires and Laurasiatheria (Table 2).

The only major order of Boreoeutheria that did not reveal evidence of a functional *Klk4* gene in the genome was Chiroptera (bats). We identified exons 4 – 6 of *Klk4* in *Rhinolophus ferrumequinum* (greater horseshoe bat) and exon 6 of this gene in *Megaderma lyra* (greater false vampire bat), but did not in eight other bat species for which the genome sequence is currently available. In fact, each of these four exons has one or more deleterious mutation (Figure S8). However, at least two different deleterious insertions/deletions were also detected in *Klk5* in greater horseshoe bat (data not shown). More accurate genome sequences are required to conclude the presence or absence of functional *Klk4* genes in bat genomes.

The Southern white rhinoceros (*Ceratotherium simum simum*), horse (*Equus caballus*), European rabbit (*Oryctolagus cuniculus*) and guinea pig (*Cavia porcellus*) genomes showed two different copies of *Klk4* . Both copies are apparently only functional in the rhinoceros, as the second copy in each of the other three species contains a premature termination codon and/or frameshift mutation. While the two copies of rhinoceros *Klk4* genes appear to maintain similar amino acid sequences (joined with small branches in Figure S5), *Klk4 - like* genes found in the chinchilla and degu genomes are significantly different from *bona fide Klk4*, as we described above (Figure S5). We assume that the many *Klk4 - like* genes in these two rodents may have obtained new functions, as these genes diverged from *bona fide Klk4* .

During analysis of the data, we considered that *Klk4* could have been present in ancestral species and then deleted in the specific afrotherian and xenarthran genomes analyzed. *Klk4* is functionally specific for dental enamel formation (Simmer et al., 2011b). This view is consistent with our analysis of *Klk4* in whales. We identified at least two apparently deleterious mutations in this gene in a baleen whale (*Balaenoptera acutorostrata scammoni;* minke whale), whereas no such mutations were detected in toothed whales, including *Orcinus orca* (killer whale) and *Tursiops truncatus* (bottlenose dolphin; Table 1 and Figure S9). Other tooth-specific genes, such *amelogenin* (*Amelx*), *enamelin* (*Enam*), *ameloblastin* (*Ambn*), and matrix *metalloproteinase 20* (*Mmp20*) also tend to be pseudogenized in species that have lost the ability to make teeth during evolution (Meredith et al., 2009, 2011, 2013). Although the enamel matrix protein genes have been pseudogenized in two xenarthran

species (Hoffmann' s two-toed sloth and the nine-banded armadillo), remnants of these genes are still evident in these genomes. In the present study, *Klk4* was not detected in the genome of these two xenarthran species or the aardvark, an enamel-less afrotherian species. Moreover, no functional *Klk4* was detected in the genomes of any of the six enamel-bearing species in Afrotheria or three species in Marsupialia, and only a fragmented pseudogene of *Klk4* was identified in the golden mole genome, whereas *Klk5* was detected in the genomes of all of these species. In addition, *Klk4* was identified in 47 species in Euarchontoglires and Laurasiatheria, the two clades of Boreoeutheria. Considering the divergence of Afrotheria, Xenarthra and Boreoeutheria in a short period of time, the phylogenetic distribution of *Klk4* suggests that the duplication that generated *Klk4* from *Klk5* most likely occurred in the common ancestor of these three groups of Eutheria and that functionally-differentiated *Klk4* survived or was selected for only in Boreoeutheria. An apparent inconsistency between this conclusion and our phylogenetic tree could be explained by a large functional divergence of *Klk4* from *Klk5* .

Exaptation for earlier eruption or enamel thickening

The finding that *Klk4* originated so recently during mammalian evolution is unexpected and intriguing. The gene encoding MMP20, the secreted protease that cleaves enamel proteins primarily during the early (secretory) stage of amelogenesis, arose before the divergence of actinopterygians (ray-finned fish) and sarcopterygians (lobe-finned fish) (Kawasaki and Suzuki, 2011). The genes encoding the secretory stage enamel matrix proteins (amelogenin, ameloblastin and enamelin) are all found in the coelacanth (lobe-finned fish) (Kawasaki and Amemiya, 2013), while none of the enamel proteins have been confirmed in teleosts (Kawasaki, 2011). Lungfish deposit thin mineral ribbons on the surface of dentin that is evocative of enamel deposition by ameloblasts during the secretory stage of amelogenesis in mammals (Satchell et al., 2000; Barry and Kemp, 2007). Thus it would appear that the fundamental mechanism of early amelogenesis is shared widely throughout extant sarcopterygians. It is the second (enamel maturation) stage that appears to have undergone the recent innovation of *KLK4* secretion. But why has this happened?

Afrotheria, and by extension the ancestral species to extant Eutheria, shows delayed eruption of their permanent teeth relative to Boreoeutheria (Asher and Lehmann, 2008). Afrotherian permanent teeth generally erupt after the individual is fully grown and sexually mature. The consequence of tooth eruption prior to enamel maturation is rapid attrition of the enamel layer, which tends to cause negative selection. The secretion of *KLK4* by maturation stage ameloblasts facilitates the removal of residual enamel proteins, which in turn accelerates the maturation or hardening of the enamel layer. With this innovation in Boreoeutheria, mutations that caused thickening of the enamel layer or earlier eruption of the permanent dentition would not have suffered rapid attrition as a consequence. Such mutations could have undergone positive selection when earlier eruption of the permanent teeth or the eruption of teeth with thicker enamel permitted the exploitation of additional dietary resources.

Materials and methods

Retrieving kallikrein gene sequences

Amino acid sequences of the 15 human *KLK* genes were retrieved from the National Center for Biotechnology Information (NCBI; http://www.ncbi.nlm.nih.gov/) and used as query sequences to search for *KLK* genes in other species at NCBI and Ensembl (http://uswest.ensembl.org/index.html), and then newly-identified *KLK* gene sequences were used to determine the gene location in its genome using the various genome sequences available at the UCSC genome browser (http://genome.ucsc.edu/index.html) and at NCBI. In addition, *Klk4* and *Klk5* were directly searched for in the genome sequence of various bat, afrotherian, xenarthran and marsupial species, as well as the chinchilla, degu and platypus. Through this process, we corrected or excluded some erroneously predicted exons from our analyses and identified many *KLK* genes, including non-functional pseudogenes, in the genome of mammals, reptiles, birds and the western clawed frog. Notably, most of these genes formed a cluster with an identical transcriptional direction, which is consistent with the interpretation that the *KLK* genes arose principally by tandem duplication. Our analysis also detected *trypsin* genes in various species, including teleostfish. Both trypsins and *KLK*s belong to the S1A serine peptidase family and are evolutionarily closely related to each other. The finding of *trypsin* genes in our study indicates an exhaustive coverage of *KLK* genes in the currently-available databases.

Constructing a phylogenetic tree

Amino acid sequences were aligned using TCOFFEE (http://www.tcoffee.org/) (Notredame, 2010). In order to obtain a reliable phylogenetic tree, our analysis used only *KLK* genes that contained the entire active protein sequence (corresponding to the trypsin-like serine protease domain) (Parry et al., 1998) with no ambiguous residues. The amino acid sequence alignment was then used to construct a phylogenetic tree using MEGA6.05 by the maximum likelihood (ML) method (Nei and Kumar, 2000; Tamura et al., 2013). For constructing ML trees, a best-fit amino acid substitution model was calculated also using MEGA6.05, and the WAG+G+I, LG +G+I, or JTT+G+I model was used (see figure legends) (Le and Gascuel, 2008; Tamura et al., 2011). All gaps in the sequence alignment were excluded from the analysis. The reliability of the interior branches was calculated by 500-time bootstrap resampling (Nei and Kumar, 2000). The amino acid sequences used in our study and their GenBank accession numbers are summarized in Table 1 and Figures S1, S2 and S7.

Analyzing functional divergence

Functional divergence of duplicate genes may be detected as two different types of amino acid configurations in a multiple sequence alignment. In type-I divergence, the amino acid sequence is highly conserved at a specific position coded by one gene, but highly variable in the other gene, or *vice versa* (Gu, 1999). In type-II divergence, the amino acid sequence is highly conserved at a specific position encoded by both genes, but the character of the coded residue is highly different between the two genes (Gu, 2006). In order to explore the degree of functional divergence between *Klk4* and *Klk5*, a multiple alignment was prepared using the amino acid sequences encoded by 38 *Klk4*, 41 *Klk5* and 10 *Klk7* genes (*Klk7* was used as the outgroup; Figure S7) and an ML tree was constructed, as stated above. Based upon the

multiple sequence alignment and the ML tree, the coefficient of type-I and type-II functional divergence (θ) between the *Klk4*, *Klk5* and *Klk7* clades was estimated using the Diverge 2.0 soft ware (Gu, 1999, 2006). This soft ware was also employed to estimate the type-I functional branch length from their common ancestral gene for each *KLK* clade (Wang and Gu, 2001), and to calculate the posterior probability of the shift in the evolutionary rate at each amino acid position (Wang and Gu, 2001).

Supplementary Material

Refer to Web version on PubMed Central for supplementary material.

Acknowledgments

This investigation was supported by USPHS Research Grant DE019775 from the National Institute of Dental and Craniofacial Research, National Institutes of Health, Bethesda, MD 29892 and National Science Foundation grants BCS0725227 and BCS0343442.

References

Asher RJ, Lehmann T. Dental eruption in afrotherian mammals. BMC Biol. 2008; 6:14. [PubMed: 18366669]

Barry JC, Kemp A. High resolution transmission electron microscopy of developing enamel in the Australian lungfish, Neoceratodus forsteri (Osteichthyes: Dipnoi). Tissue Cell. 2007; 39:387–398. [PubMed: 17888476]

Deakins M, Volker JF. Amount of organic matter in enamel from several types of human teeth. J. Dent. Res. 1941; 20:117–121.

Elliott MB, Irwin DM, Diamandis EP. In silico identification and Bayesian phylogenetic analysis of multiple new mammalian kallikrein gene families. Genomics. 2006; 88:591–599. [PubMed: 16829021]

Fukae M, Shimizu M. Studies on the proteins of developing bovine enamel. Arch. Oral Biol. 1974; 19:381–386. [PubMed: 4527995]

Gu X. Statistical methods for testing functional divergence after gene duplication. Mol. Biol. Evol. 1999; 16:1664–1674. [PubMed: 10605109]

Gu X. A simple statistical method for estimating type-II (cluster-specific) functional divergence of protein sequences. Mol. Biol. Evol. 2006; 23:1937–1945. [PubMed: 16864604]

Hart PS, Hart TC, Michalec MD, Ryu OH, Simmons D, Hong S, Wright JT. Mutation in kallikrein 4 causes autosomal recessive hypomaturation amelogenesis imperfecta. J. Med. Genet. 2004; 41:545–549. [PubMed: 15235027]

Hu JC, Zhang C, Sun X, Yang Y, Cao X, Ryu O, Simmer JP. Characterization of the mouse and human PRSS17 genes, their relationship to other serine proteases, and the expression of PRSS17 in developing mouse incisors. Gene. 2000; 251:1–8. [PubMed: 10863090]

Hu JC, Sun X, Zhang C, Liu S, Bartlett JD, Simmer JP. Enamelysin and kallikrein-4 mRNA expression in developing mouse molars. Eur. J. Oral Sci. 2002; 110:307–315. [PubMed: 12206593]

Hu Y, Hu JC, Smith CE, Bartlett JD, Simmer JP. Kallikrein-related peptidase 4, matrix metalloproteinase 20, and the maturation of murine and porcine enamel. Eur. J. Oral Sci. 2011; 119:217–25. [PubMed: 22243249]

Kawasaki K. The SCPP gene family and the complexity of hard tissues in vertebrates. Cells Tissues Organs. 2011; 194:108–112. [PubMed: 21576905]

Kawasaki K, Amemiya C. SCPP genes in the coelacanth: Tissue mineralization genes shared by sarcopterygians. J. Exp. Zool. (Mol. Dev. Evol.). 2013; 9999B:1–13.

Kawasaki K, Suzuki T. Molecular evolution of matrix metalloproteinase 20. Eur. J. Oral Sci. 2011; 119:247–253. [PubMed: 22243253]

Klein SL, Strausberg RL, Wagner L, Pontius J, Clifton SW, Richardson P. Genetic and genomic tools for Xenopus research: The NIH Xenopus initiative. Dev. Dyn. 2002; 225:384–391. [PubMed: 12454917]

Koumandou VL, Scorilas A. Evolution of the plasma and tissue kallikreins, and their alternative splicing isoforms. PLoS One. 2013; 8:e68074. [PubMed: 23874499]

Le SQ, Gascuel O. An improved general amino acid replacement matrix. Mol. Biol. Evol. 2008; 25:1307–1320. [PubMed: 18367465]

Lu Y, Papagerakis P, Yamakoshi Y, Hu JC, Bartlett JD, Simmer JP. Functions of *KLK4* and MMP-20 in dental enamel formation. Biol. Chem. 2008; 389:695–700. [PubMed: 18627287]

Lundwall A. Old genes and new genes: the evolution of the kallikrein locus. Thromb. Haemost. 2013; 110:469–475. [PubMed: 23571662]

Meredith RW, Gatesy J, Murphy WJ, Ryder OA, Springer MS. Molecular decay of the tooth gene Enamelin (ENAM) mirrors the loss of enamel in the fossil record of placental mammals. PLoS Genet. 2009; 5:e1000634. [PubMed: 19730686]

Meredith RW, Gatesy J, Cheng J, Springer MS. Pseudogenization of the tooth gene enamelysin (MMP20) in the common ancestor of extant baleen whales. Proc. Biol. Sci. 2011; 278:993–1002. [PubMed: 20861053]

Meredith RW, Gatesy J, Springer MS. Molecular decay of enamel matrix protein genes in turtles and other edentulous amniotes. BMC Evol Biol. 2013; 13:20. [PubMed: 23342979]

Nagano T, Kakegawa A, Yamakoshi Y, Tsuchiya S, Hu JC, Gomi K, Arai T, Bartlett JD, Simmer JP. Mmp-20 and *Klk4* cleavage site preferences for amelogenin sequences. J. Dent. Res. 2009; 88:823–828. [PubMed: 19767579]

Nanci, A. Enamel: composition, formation, and structure. In: Nanci, A., editor. Ten Cate ' s Oral Histology Development, Structure, and Function. St. Louis, MO: Mosby; 2003. p. 145-191.

Nei, M.; Kumar, S. Molecular Evolution and Phylogenetics. New York, NY: Oxford University Press; 2000.

Newbrun E, Pigman W. The hardness of enamel and dentine. Aust. Dent. J. 1960; 5:210–217.

Notredame C. Computing multiple sequence/structure alignments with the T-coffee package. Curr. Protoc. Bioinformatics. 2010 *Chapter*, Unit 3.8.1-25.

Ohno, S. Evolution by Gene Duplication. New York, NY: Springer; 1970.

Parry MA, Fernandez-Catalan C, Bergner A, Huber R, Hopfner KP, Schlott B, Gührs KH, Bode W. The ternary microplasmin-staphylokinase-microplasmin complex is a proteinase-cofactor-substrate complex in action. Nat. Struct. Biol. 1998; 5:917–923. [PubMed: 9783753]

Pavlopoulou A, Pampalakis G, Michalopoulos I, Sotiropoulou G. Evolutionary history of tissue kallikreins. PLoS One. 2010; 5:e13781. [PubMed: 21072173]

Ryu OH, Hu CC, Zhang C, Qian Q, Moradian-Oldak J, Fincham AG, Simmer JP. Proteolytic activity of opossum tooth extracts. Eur. J. Oral Sci. 1998; 106(Suppl 1):337–344. [PubMed: 9541245]

Ryu O, Hu JC, Yamakoshi Y, Villemain JL, Cao X, Zhang C, Bartlett JD, Simmer JP. Porcine kallikrein-4 activation, glycosylation, activity, and expression in prokaryotic and eukaryotic hosts. Eur. J. Oral Sci. 2002; 110:358–365. [PubMed: 12664466]

Satchell PG, Shuler CF, Diekwisch TG. True enamel covering in teeth of the Australian lungfish Neoceratodus forsteri. Cell Tissue Res. 2000; 299:27–37. [PubMed: 10654067]

Simmer JP, Hu Y, Lertlam R, Yamakoshi Y, Hu JC. Hypomaturation enamel defects in *Klk4* knockout/LacZ knockin mice. J. Biol. Chem. 2009; 284:19110–19121. [PubMed: 19578120]

Simmer J, Hu Y, Richardson A, Bartlett J, Hu JC-C. Why does enamel in *Klk4* null mice break above the dentinoenamel junction ? Cells Tissues Organs. 2011a; 194:211–215. [PubMed: 21546759]

Simmer JP, Richardson AS, Smith CE, Hu Y, Hu JC. Expression of kallikrein-related peptidase 4 in dental and non-dental tissues. Eur. J Oral Sci. 2011b; 119:226–233. [PubMed: 22243250]

Smith CE. Cellular and chemical events during enamel maturation. Crit. Rev. Oral Biol. Med. 1998; 9:128–161. [PubMed: 9603233]

Smith CE, Richardson AS, Hu Y, Bartlett JD, Hu JC, Simmer JP. Effect of Kallikrein 4 loss on enamel mineralization: comparison with mice lacking matrix metalloproteinase 20. J. Biol. Chem. 2011; 286:18149–18160. [PubMed: 21454549]

Tamura K, Peterson D, Peterson N, Stecher G, Nei M, Kumar S. MEGA5: molecular evolutionary genetics analysis using maximum likelihood, evolutionary distance, and maximum parsimony methods. Mol. Biol. Evol. 2011; 28:2731–2739. [PubMed: 21546353]

Tamura K, Stecher G, Peterson D, Filipski A, Kumar S. MEGA6: Molecular Evolutionary Genetics Analysis version 6.0. Mol. Biol. Evol. 2013; 30:2725–2729. [PubMed: 24132122]

Wang Y, Gu X. Functional divergence in the caspase gene family and altered functional constraints: statistical analysis and prediction. Genetics. 2001; 158:1311–1320. [PubMed: 11454777]

Wang SK, Hu Y, Simmer JP, Seymen F, Estrella NM, Pal S, Reid BM, Yildirim M, Bayram M, Bartlett JD, et al. Novel *KLK4* and MMP20 mutations discovered by whole-exome sequencing. J. Dent. Res. 2013; 92:266–271. [PubMed: 23355523]

Wong MK, Takei Y. Lack of plasma kallikrein-kinin system cascade in teleosts. PLoS One. 2013; 8:e81057. [PubMed: 24278376]

Yamakoshi Y, Richardson AS, Nunez SM, Yamakoshi F, Milkovich RN, Hu JC, Bartlett JD, Simmer JP. Enamel proteins and proteases in Mmp20 and *Klk4* null and double-null mice. Eur. J. Oral Sci. 2011; 119:206–216. [PubMed: 22243248]

Yousef GM, Chang A, Scorilas A, Diamandis EP. Genomic organization of the human kallikrein gene family on chromosome 19q13.3-q13.4. Biochem. Biophys. Res. Commun. 2000; 276:125–133. [PubMed: 11006094]

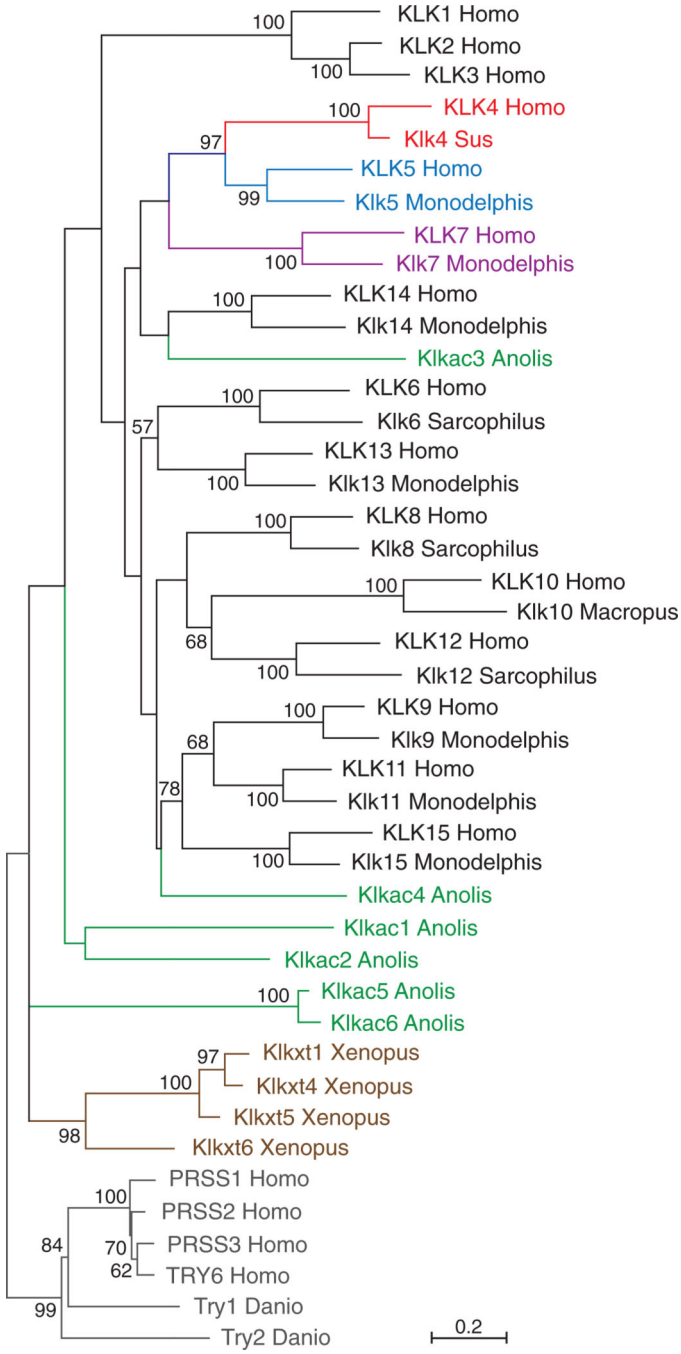

Figure 1.

Phylogenetic tree of the *KLK* genes. This tree was constructed by the ML method based on the WAG +G +I amino acid substitution model using MEGA6.05. Human (*PRSS1 – PRSS3* add *TRY6*) and zebrafish (*Try1* and *Try2*) *trypsin* genes served as the outgroup. The numbers at the nodes correspond to the bootstrap support (values >50% are shown). The scale was shown at the bottom. Note that 11 of the 15 human *KLK*s (*KLK5 – KLK15*) have a marsupial ortholog with high statistical support (99 – 100 %).

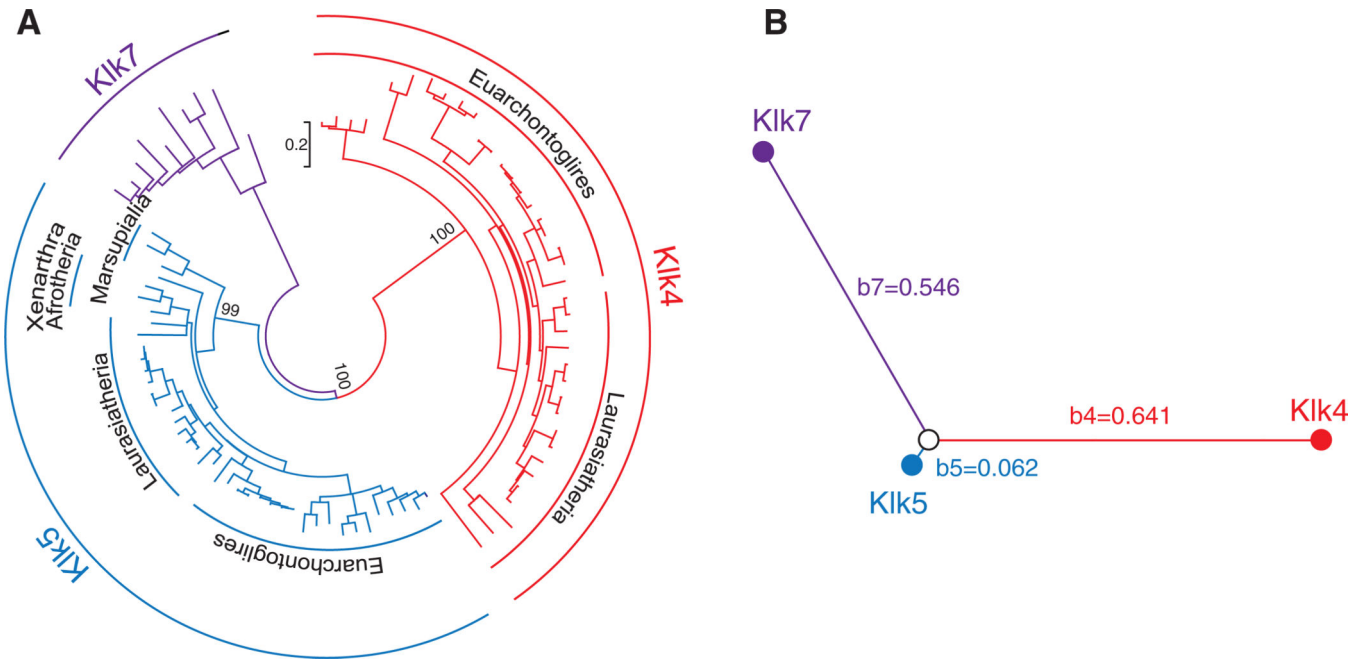

Figure 2.

Phylogenetic tree of the *Klk4*, *Klk5* and *Klk7* genes (A) and the type-I functional branch lengths of these genes (B). (A) This tree was constructed by the ML method based on the JTT+G+I amino acid substitution model. The branches to *Klk4* (Euarchontoglires and Laurasiatheria), *Klk5* (Euarchontoglires, Laurasiatheria, Xenarthra/Afrotheria and Marsupialia) and *Klk7* are supported by a bootstrap value of 99–100%. The scale is shown between *Klk4* and *Klk7*. (B) The type-I branch lengths of each *KLK* gene cluster from their common ancestral gene, calculated using Diverge 2.0 (b4 = 0.641, b5 = 0.062, and b7 = 0.546), are illustrated. Note that b5 is much shorter than b4 (and b7), suggesting a functional divergence of *Klk4* from *Klk5*.

Table 1

Klk4 and *Klk5* in mammals

Eutheria		
Boreoeutheria		
Euarchontoglires		
Primates		
Homosapience	NP_004908.3	NP_036559.1
Pantroglodytes	XP_524486.2	XP_003316612.1
Pan paniscus	XP_003813692.1	XP_003813725.1
Gorilla gorillagorilla	XP_004061306.1	XP_004061310.1
Pongo abelii	XP_003779284.1	XP_002829673.1
Nomascus leucogenys	XP_003269865.1	XP_003269866.1
Macaca mulatta	XP_001118233.1	NP_001248026.1
Macaca fascicularis	XP_005590110.1	XP_005590111.1
Papio anubis	XP_003916026.1	XP_003916027.1
Saimiri boliviensis boliviensis	XP_003940460.1	XP_003940461.1
Callithrix jacchus	XP_002762457.2	Exons 1–3 and 6 detected
Otolemur garnettii	XP_003803290.1	XP_003803279.1
Scandentia		
Tupaia chinensis	XP_006144757.1	XP_006144758.1
Rodentia		
Mus musculus	NP_064312.1	NP_081082.1
Rattus norvegicus	NP_001004101.1	XP_006223315.1
Cricetulus griseus	XP_003510254.1	XP_003510253.1
Cavia porcellus	XP_003465453.1	ND
Ictidomys tridecemlineatus	XP_005341744.1	XP_005341729.1
Heterocephalus glaber	XP_004866840.1	XP_004866839.1
Microtus ochrogaster	XP_005366948.1	XP_005366949.1
Jaculus jaculus	XP_004672626.1	XP_004672635.1
Chinchilla lanigera	XP_005412785.1	XP_005412784.1
Octodon degus	XP_004644690.1	XP_004644712.1
Mesocricetus auratus	XP_005084894.1	XP_005084895.1
Lagomorpha		
Oryctolagus cuniculus	XP_002724044.1; XP_002724046.1	XP_002724045.1
Ochotona princeps	XP_004597006.1	XP_004597005.1
Laurasiatheria		
Cetartiodactyla		
Sus scrofa	NP_998967.1	HX228705.1 (EST)
Bos taurus	NP_001192550.1	NP_001193209.1
Bos mutus	XP_005898491.1	XP_005898503.1
Ovis aries	XP_004015454.1	XP_004015445.1

Eutheria		
Boreoeutheria		
Euarchontoglires		
Capra hircus	XP_005692803.1	XP_005692805.1
Pantholops hodgsonii	XP_005955484.1	XP_005955485.1
Camelus ferus	XP_006174346.1	XP_006174369.1
Vicugna pacos	XP_006208485.1	XP_006208708.1
Tursiops truncatus	XP_004324273.1	XP_004324275.1
Orcinus orca	XP_004286175.1	XP_004286174.1
Balaenoptera acutorostrata scammoni	exons 2, 4–6 detected	XP_007180015.1
Perissodactyla		
Equus caballus	XP_001497570.2; XP_005614830.1	XP_005596488.1
Ceratotherium simum simum	XP_004440495.1; XP_004440386.1	XP_004440388.1
Carnivora		
Canis lupus familiaris	NP_001184098.1	NP_001184096.1
Felis catus	XP_003997525.1	XP_003997529.1
Mustela putorius furo	XP_004767227.1	XP_004767226.1
Ailuropoda melanoleuca	XP_002929828.1	XP_002929827.1
Odobenus rosmarus divergens	XP_004410000.1	XP_004410002.1
Chiroptera		
Myotis davidii	ND	ELK30145.1
Myotis brandtii	ND	XP_005879701.1
Rhinolophus ferrumequinum	Exons 4–6detected	Exons 2–6detected
Megaderma lyra	Exon 6 detected	Exons 4–6detected
Eulipotyphla		
Erinaceus europaeus	ENSEEUP00000011954.1 (Ensembl)	ND
Sorex araneus	XP_004619931.1	XP_004619932.1
Condylura cristata	XP_004694371.1	XP_004694098.1
Xenarthra		
Cingulata		
Dasypus novemcinctus	ND	XP_004466586.1
Pilosa		
Choloepus hoffmanni	ND	Exon 5 detected
Afrotheria		
Afrosoricida		
Echinops telfairi	ND	XP_004710753.1
Chrysochloris asiatica	Exons 4–6detected	XP_006868436.1
Macroscelidea		
Elephantulus edwardii	ND	XP_006897345.1
Tublidentata		
Orycteropus afer	ND	ENSP00000337733.1 (Ensembl)

Eutheria		
Boreoeutheria		
Euarchontoglires		
Proboscidea		
Loxodonta africana	ND	Exons 3–6detected
Hyracoidea		
Procavia capensis	ND	Exons 2–6detected
Sirenia		
Trichechus manatus latirostris	ND	XP_004381774.1
Marsupialia		
Monodelphis domestica	ND	XP_001366980.1
Macropus eugenii	ND	ENSMEUP00000000346.1 (Ensembl)
Sarcophilus harrisii	ND	XP_003765290.1
Monotremata		
Ornithorhynchus anatinus	ND	(XP_001521228.1[a])

[a]This sequence was not firmly confirmed as *Klk5* by phylogenetic analysis because of its small size (44 amino acids). However, highest scores by a Blast search were obtained for *Klk5* sequences from various mammals.

Table 2

θ values from pairwise comparisons between *Klk4*, *Klk5* and *Klk7*.

	Klk4	***Klk5***	***Klk7***
Klk4		0.555	0.664
Klk5	0.040		0.458
Klk7	0.048	0.042	

The upper diagonal shows the pairwise θ values, and the lower diagonal shows the standard errors.